Mode-specific energy absorption by solvent molecules during CO_2 vibrational cooling

Alexander Kandratsenka,*[a] Jörg Schroeder,[a] Dirk Schwarzer[a] and Vyacheslav S. Vikhrenko[b]

Received 18th December 2006, Accepted 1st February 2007
First published as an Advance Article on the web 23rd February 2007
DOI: 10.1039/b618452a

Non-equilibrium molecular dynamics (NEMD) simulations of energy transfer from vibrationally excited CO_2 to CCl_4 and CH_2Cl_2 solvent molecules are performed to identify the efficiency of different energy pathways into the solvent bath. Studying in detail the work performed by the vibrationally excited solute on the different solvent degrees of freedom, it is shown that vibration-to-vibration (V–V) processes are strongly dominant and controlled by those accepting modes which are close in frequency to the CO_2 bend and symmetric stretch vibration.

1. Introduction

Unravelling the mechanisms and pathways by which vibrational energy is redistributed in excited polyatomic molecules and exchanged with the surrounding medium is an important prerequisite for understanding chemical reaction dynamics. Therefore, over the last decades vibrational energy relaxation (VER) processes have been studied extensively and are still of major current interest.[1–16] Both, experimental and theoretical efforts were mainly concentrated on the excited solute itself by analysing how the excess vibrational energy migrates inside the activated molecule from mode to mode and is finally transferred to the surrounding bath. Less attention was paid to a detailed analysis of how polyatomic bath molecules gain the energy from the solute, *i.e.* to the question of how the energy flux from the solute is partitioned into translational, rotational and vibrational degrees of freedom of the solvent molecules. Experimentally some insight into this issue was obtained by measuring thermal heating of the solvent following vibrational energy transfer using the transient grating method[17,18] and by observing the excitation of low frequency modes of CCl_4 during vibrational relaxation of methanol[19,20] and nitromethane,[11] respectively. Since a rigorous quantum mechanical treatment of this problem is not feasible, theoretical studies analysing the energy gain of the solvent during VER rely on classical molecular dynamics (MD) calculations. The approaches employed are using either nonequilibrium (NEMD)[21] or equilibrium (EMD) molecular dynamics simulations, the latter within a perturbative treatment of solvent solute coupling.[2,22,23]

Recently, we performed EMD and NEMD calculations to elucidate the relaxation mechanism of vibrationally excited CO_2 in CH_2Cl_2, CCl_4, and xenon.[24] This work was motivated by time-resolved photodissociation experiments on organic peroxides,[25] which after UV-excitation undergo O–O bond breakage on a femtosecond time-scale generating 'hot' aroyloxy radicals. These fragments further decompose to form vibrationally highly excited CO_2, whose subsequent VER was measured by following the temporal evolution of the transient IR-absorption of the CO_2 ν_3-band (asymmetric stretch, 2390 cm^{-1}).[26–28]

Our MD simulations show[24] that due to strong Fermi resonance the symmetric stretching (ν_1 = 1350 cm^{-1}) and bending (ν_2 = 670 cm^{-1}) vibrations of CO_2 in CH_2Cl_2 and CCl_4 jointly relax on a ten and hundred picosecond timescale, respectively, in accordance with experiment. The high frequency CO_2 asymmetric stretch vibration, however, only weakly interacts with both the other modes and the bath degrees of freedom and, therefore, independently relaxes on a much longer time-scale. The dominant relaxation channel is the low frequency bending vibration. In CCl_4 and xenon almost 100% of the excess energy is transferred *via* this channel, in CH_2Cl_2 it is 73%. In contrast to xenon where the relaxation takes 20 ns, the short VER times in CH_2Cl_2 and CCl_4 are caused by efficient near resonant vibration to vibration (V–V) energy transfer. This interpretation is supported by analysing the power spectra of external solvent forces acting on the CO_2 bending and symmetric stretch vibrations as presented in Fig. 1. According to Landau–Teller theory the amplitude of these spectra at the frequency of the considered normal mode is a direct measure of the VER rate constant. Whereas for xenon slightly stretched exponential decays are found, the spectra of CH_2Cl_2 and CCl_4 in Fig. 1 are structured by pronounced resonant features arising from vibrational modes of the solvent. The overlap of CO_2 vibrational frequencies with these resonances indicates efficient V–V energy transfer.

Although the relaxation channels of the solute can be quantified by the spectra of Fig. 1 in great detail, the corresponding analysis for the solvent molecules is possible only in a qualitative fashion. For example, the spectrum of CCl_4 forces acting on the CO_2 bend vibration in Fig. 1b indicates a close resonance between ν_2 and the 776 cm^{-1} CCl asymmetric stretch mode suggesting that this solvent mode is an important relaxation channel. However, the precise contribution of the CCl stretch, the partitioning of the energy flow out

[a] *Abteilung Spektroskopie und Photochemische Kinetik, Max-Planck-Institut für Biophysikalische Chemie, Am Faßberg 11, D-37077 Göttingen, Germanyand Institut für Physikalische Chemie, Universität Göttingen, Tammanstraße 6, 37077 Göttingen, Germany. E-mail: akandra@gwdg.de*
[b] *Department of Theoretical Mechanics, Belarusian State Technological University, Sverdlova str. 13a, 220050 Minsk, Belarus. E-mail: vvikhre@mail.ru*

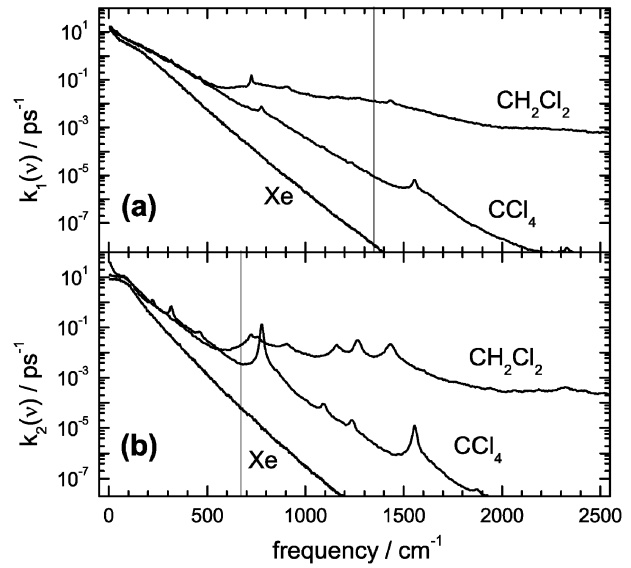

Fig. 1 The frequency dependent VER rate constants (LT approach) of (a) symmetric stretch and (b) bend vibrational modes of CO_2 in different solvents. Additional vertical lines indicate the CO_2 fundamental frequencies.

of the CO_2 bending vibration into translational, rotational, and possibly other accepting vibrational modes of the bath cannot be derived from Fig. 1.

In order to get just this information we performed additional NEMD simulations of the vibrational relaxation of CO_2 in CCl_4 and CH_2Cl_2. The energy accepting bath degrees of freedom are determined by calculating the work performed by the excited CO_2 molecule on the solvents normal modes as well as its translational and rotation motions during relaxation.

2. Theoretical background

The energy pathways into the solvent can be analysed by studying the work performed by the vibrationally excited solute on different solvent degrees of freedom. To this end it is necessary to consider the interplay between energy changes of the subsystems and works performed by the underlying forces.

The total energy of the system can be represented as a sum of three terms

$$E = E_{\mathrm{v}} + E_{\mathrm{b}} + E_{\mathrm{vb}}, \qquad (1)$$

where E_{v}, E_{b} and E_{vb} are the energies of the vibrationally excited solute, the solvent (bath) and the solute–solvent interaction, respectively. In the NVE ensemble the total energy is conserved. Thus, the sum of energy variations of the contributions in eqn (1) is equal to zero

$$\Delta E_{\mathrm{v}} + \Delta E_{\mathrm{b}} + \Delta E_{\mathrm{vb}} = 0. \qquad (2)$$

Eqns (1) and (2) are correct for each MD trajectory as well as for averages over an ensemble of trajectories. In the latter case the solute–solvent interaction energy does not strongly depend on the vibrational state of the solute so that $\Delta E_{\mathrm{vb}} \approx 0$. Thus, the energy released from the solute is approximately equal to the energy absorbed by the solvent, *i.e.* $\Delta E_{\mathrm{v}} \approx -\Delta E_{\mathrm{b}}$. The energy absorbed by the bath can be partitioned into external translational and rotational as well as internal vibrational degrees of freedom of solvent molecules. The character of this partitioning is the object of this investigation.

For a quantitative description of the energy exchange channels it is useful to introduce the concept of mode specific work:[29,30] The energy variation of a system is equal to the work performed by external forces. The latter can be calculated from time integrals of the corresponding force capacities. For the solute and solvent subsystems the following expressions apply

$$\Delta E_{\mathrm{v}} = \int_0^t \left(\sum_{i=1}^{m_{\mathrm{v}}} \sum_{j=1}^{M_{\mathrm{b}}} \boldsymbol{F}_{ij} \cdot \boldsymbol{v}_i \right) \mathrm{d}t, \quad M_{\mathrm{b}} = M m_{\mathrm{b}}, \qquad (3)$$

$$\Delta E_{\mathrm{b}} = \int_0^t \left(\sum_{i=1}^{m_{\mathrm{v}}} \sum_{j=1}^{M_{\mathrm{b}}} \boldsymbol{F}_{ji} \cdot \boldsymbol{v}_j \right) \mathrm{d}t, \qquad (4)$$

where m_{v} and m_{b} are the number of atoms of the solute and solvent molecules, respectively, and M is the number of solvent molecules. $\boldsymbol{F}_{ij}$ is the force exerted on atom i by atom j.

In accordance with the law of action and reaction $\boldsymbol{F}_{ij} = -\boldsymbol{F}_{ji}$. Then the sum of eqn (2) and (3) can be written as

$$\Delta E_{\mathrm{v}} + \Delta E_{\mathrm{b}} = \int_0^t \left(\sum_{i=1}^{m_{\mathrm{v}}} \sum_{j=1}^{M_{\mathrm{b}}} \boldsymbol{F}_{ij} \cdot (\boldsymbol{v}_i - \boldsymbol{v}_j) \right) \mathrm{d}t. \qquad (5)$$

It is necessary to note that eqn (5) is invariant with respect to the coordinate system used (*i.e.* to changes of the velocities by a constant), while eqn (3) and (4) do not satisfy this condition. However, for coordinate systems utilized in common MD simulations the total momentum of the solute + solvent system is equal to zero and both eqn (3) and (4) exactly describe the energy variations of the subsystems.

The capacity N_j of the force $\mathbf{F}_j = \sum_{i=1}^{n_{\mathrm{v}}} \boldsymbol{F}_{ji}$ exerted on the j-th atom of a solvent molecule by the solute is calculated *via*

$$N_j = \boldsymbol{F}_j \cdot (\boldsymbol{v}_{\mathrm{C}} + \boldsymbol{\omega} \times \boldsymbol{r}_j + \boldsymbol{u}_j) \qquad (6)$$

where $\boldsymbol{v}_{\mathrm{C}}$ and $\boldsymbol{\omega}$ are the center of mass and angular velocities of the molecule, respectively, $\boldsymbol{r}_j$ is the position vector of atom j with respect to the molecular center of mass C and $\boldsymbol{u}_j$ is vibrational velocity of atom j. After summation over all the atoms of a solvent molecule one gets

$$N = \boldsymbol{R} \cdot \boldsymbol{v}_{\mathrm{C}} + \boldsymbol{M}_{\mathrm{C}} \cdot \boldsymbol{\omega} + \sum_j \boldsymbol{F}_j \cdot \boldsymbol{u}_j \qquad (7)$$

where $\boldsymbol{R} = \sum_j \boldsymbol{F}_j$ and $\boldsymbol{M}_{\mathrm{C}} = \sum_j (\boldsymbol{r}_j - \boldsymbol{r}_{\mathrm{C}}) \times \boldsymbol{F}_j$ represent the sum of forces and their torques with respect to the centre of mass, respectively. The angular velocity as well as the vibrational velocities depend on the applied molecular frame. In the Eckart frame[31,32] used below the rotation–vibration interaction is minimized.

For a mode specific analysis it is more informative to represent the last term of eqn (7) through normal forces Q_k (calculated from sum of external forces $\boldsymbol{F}_j$ projected on the molecular normal mode vectors) and normal mode velocities $\dot{q}_k$

$$N_{\mathrm{vibr}} = \sum_{k=1}^{s} N_k, \quad N_k = Q_k \dot{q}_k. \qquad (8)$$

N_k represents the energy flow into the k-th vibrational mode of the solvent molecule. The total energy transferred into a

molecule through a particular vibrational mode is calculated by integrating the corresponding capacity over time

$$W_k = \int_0^t N_k(t)\mathrm{d}t. \qquad (9)$$

As a consequence of the nonlocality of the potential energy (which depends on the positions of at least two particles), the momentum and angular momentum of each pair of molecules are not conserved during a MD trajectory. The outcome of these two quantities, however, determines the energy transfer to translational (V–T) and rotational (V–R) degrees of freedom of a solvent molecule. Thus, the V–T and V–R energy transfer components from the excited CO_2 to a solvent molecule are ambiguous and only after averaging over many trajectories these quantities can be calculated.

3. Simulation details

The intra- and intermolecular interaction potentials of CO_2, CCl_4 and CH_2Cl_2 used in our calculations are given in ref. 24. The CO_2 intramolecular potential was derived from spectroscopic data and contains terms up to sixth order. This ensures realistic intramolecular vibrational energy redistribution which is important for the energy transfer mechanism. More simple harmonic potentials represented in symmetry coordinates were used for the solvents CCl_4 and CH_2Cl_2. As each solvent molecule accumulates only a small amount of vibrational energy, anharmonic terms in the potential are of minor importance for the energy transfer process. The interaction energies between atoms of different molecules are modeled by sums of Lennard-Jones and Coulomb potentials. The parameters are summarized in Table 1 of ref. 24.

Nonequilibrium MD simulations of a single CO_2 molecule in a bath of 40 CH_2Cl_2 or CCl_4 molecules were performed within the NVE ensemble at $T = 300$ K. In the first 5 ps velocities were rescaled to bring the system to the desired temperature. Then 100 ps were given for equilibration of the system and after each 5 ps samples were selected for subsequent nonequilibrium simulations. Our earlier simulations have shown[24] that with respect to energy exchange the asymmetric stretch mode of CO_2 is inactive on the time-scale of several hundred picoseconds, while the energy exchange between the other two modes is very fast, *i.e.* it is not important how vibrational energy is initially distributed among them. Therefore the simulation started by adding 96.7 kJ mol^{-1} of kinetic energy equally to the symmetric stretch and bend modes of CO_2, whereas the asymmetric stretch vibration was not excited.

The length of trajectories was chosen to cover the whole relaxation process with a time increment of integration dictated by the highest vibrational frequency. For CH_2Cl_2 (CCl_4) the total simulation time was 250 ps (1 ns), the time increment was 0.25 fs (0.5 fs). The work done by the solute (CO_2) on the solvent vibrational modes [eqn (9)] was summed over all solvent molecules. The results were averaged over 194 trajectories.

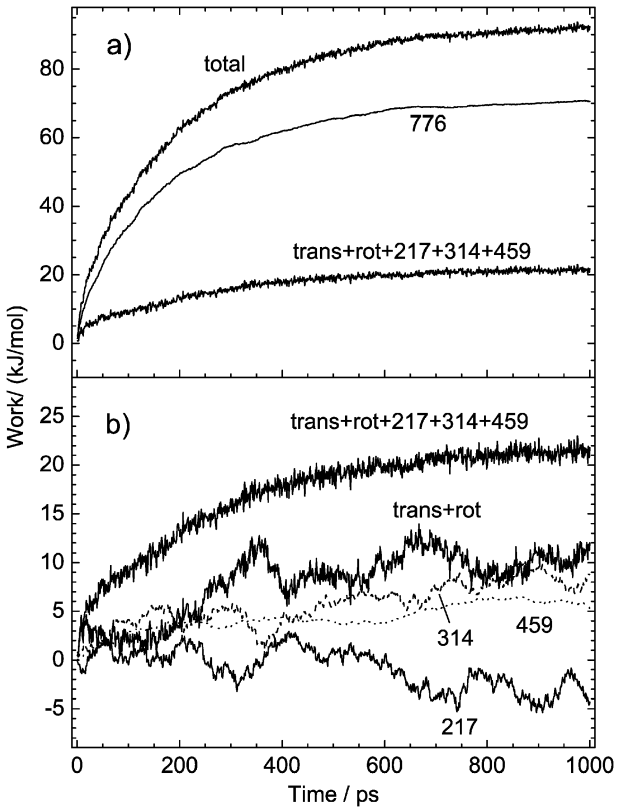

Fig. 2 Work performed to individual CCl_4 solvent modes during vibrational energy relaxation of CO_2 (CCl_4 vibrational frequencies are given in cm^{-1}); (a) indicates the 776 cm^{-1} C–Cl asymmetric stretch mode as the dominant energy accepting vibration, exponential fitting to the total work yields a time constant of (210 ± 5) ps; (b) the contribution of translation, rotation, and low frequency vibrations to the energy transfer.

4. Results and discussion

As described in our previous paper,[24] vibrationally excited CO_2 transfers all the excess energy to the CCl_4 solvent *via* its bending mode. Fig. 2 shows how this energy is partitioned into the different solvent degrees of freedom. Here, the work performed by the CO_2 molecule on the individual CCl_4 modes is plotted. Almost 80% of the total energy flows into the threefold degenerate 776 cm^{-1} CCl asymmetric stretch vibration (Fig. 2a). The remaining energy is accepted by the low frequency modes at 217 (bend), 314 (bend) and 459 cm^1 (symmetric stretch) and the translations and rotations. This result supports our initial assumption that due to close resonance to the CO_2 bend vibration at 672 cm^{-1} (as exemplified in the Landau–Teller spectrum of Fig. 1b) the 776 cm^{-1} C–Cl stretch mode provides an efficient energy transfer channel. Fitting a single exponential function of the form

$$W(t) = W_{\max}(1 - \exp(-t/\tau)) \qquad (10)$$

to the time evolution of the total work yields a time constant of $\tau = (210 \pm 5)$ ps which is in good agreement with the experimentally observed vibrational cooling time[28] of 200 ps. (In our previous paper[24] the Ewald summation for the system CO_2/CCl_4 was implemented incorrectly. The actual

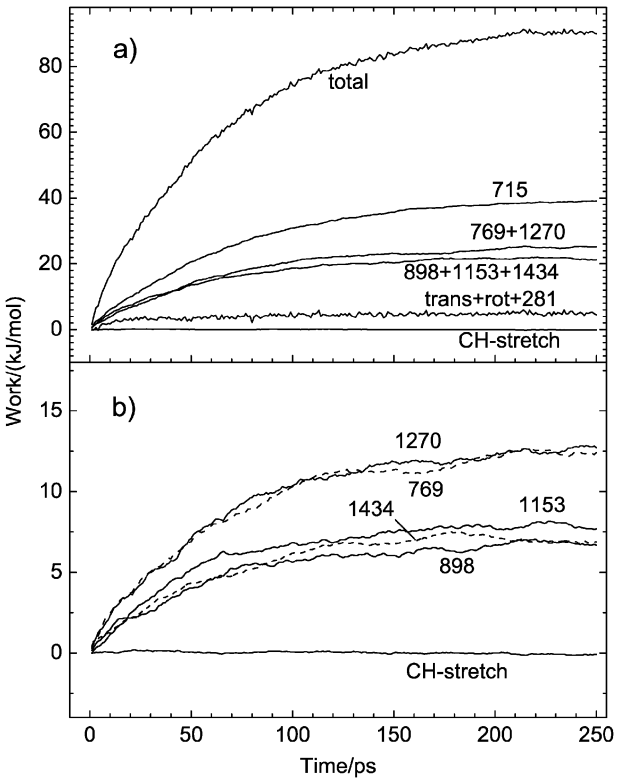

Fig. 3 Work performed to individual CH_2Cl_2 solvent modes during vibrational energy relaxation of CO_2 (CH_2Cl_2 vibrational frequencies are given in cm^{-1}); (a) indicates the 715 cm^{-1} CCl_2 symmetric stretch mode as the dominant energy accepting vibration, exponential fitting to the total work yields a time constant of (64 ± 3) ps; (b) the contribution of medium to high frequency vibrations to the energy transfer.

vibrational energy transfer time of CO_2 in this solvent is 210 ps instead of 344 ps. All other conclusions derived in ref. 24 remain the same, in particular the fact that all the excess energy of CO_2 is transferred *via* the bend vibration to the CCl_4 solvent.)

Fig. 2b focuses on the contribution of CCl_4 translational, rotational and low frequency vibrational degrees of freedom to the energy transfer. Whereas the individual components strongly fluctuate, the sum represents a relatively smooth curve. The fluctuations between translation, rotation and the low frequency vibrations is highly correlated indicating a strong coupling between these modes. Despite the fluctuations it is possible to estimate the energy transmitted into translations and rotations of the solvent to be about 10% of the total CO_2 vibrational energy. This is in a good agreement with the results shown in Fig. 9 of ref. 24 that indicate an order of magnitude difference in relaxation rates of carbon dioxide in flexible and rigid carbon tetrachloride.

In Fig. 3 the work done by the CO_2 molecule on the solvent CH_2Cl_2 is shown. The main energy transfer channel into dichloromethane is the CCl_2 symmetric stretch vibration at 715 cm^{-1}. Almost 45% of the total vibrational energy released from carbon dioxide is transferred into this mode. Again, this mode is in close resonance to the CO_2 bending vibration. 50% of energy is transferred to CH_2Cl_2 modes with frequencies in the range 769–1434 cm^{-1}. The lowest frequency CCl_2 scissor mode (281 cm^{-1}) is strongly coupled with translational and rotational degrees of freedom. Their sum contributes with 5% to the energy transfer, whereas the high-frequency CH-stretch modes are not involved in energy transfer and don't accept any energy.

Fitting eqn (10) to the time evolution of the total work in Fig. 3a yields a time constant of $\tau = (64 \pm 3)$ ps, which agrees with the experimental value of 70 ps.[28]

It was shown in our previous paper[24] that 27% of the CO_2 vibrational energy escapes through the symmetric stretch mode at 1352 cm^{-1}. Due to Fermi resonance with the bend overtone the symmetric stretch spectrum is split into two branches covering a broad range between 1250 and 1450 cm^{-1} (see Fig. 5 in ref. 24). Three CH_2Cl_2 vibrations are in close resonance with this spectrum: the CH_2 scissor mode at 1434 cm^{-1}, the CH_2 twist mode at 1153 cm^{-1}, and the CH_2 wagging mode at 1270 cm^{-1}. According to Fig. 3b these modes absorb 30% of energy suggesting that the vibrational energy released by the CO_2 symmetric stretch is gathered just by these three solvent modes. The 898 cm^{-1} CH_2 rocking and the 769 cm^{-1} CCl_2 asymmetric stretching modes of dichloromethane probably interact with the CO_2 bend vibration and gain in all 20% of the excess energy.

5. Conclusions

Nonequilibrium MD simulations provide a detailed view into the energy pathways during vibrational energy relaxation of CO_2 in CCl_4 and CH_2Cl_2 solvents. For both solvents the relaxation is dominated by V–V energy transfer. In CCl_4 all the excess energy leaves the CO_2 molecule *via* its bend vibration (670 cm^{-1}). 80% of this energy is accepted by the CCl asymmetric stretch vibration at 776 cm^{-1}. The rest flows into low frequency vibrations, only a minor part to translational and rotational degrees of freedom of the bath.

In CH_2Cl_2 only 73% of the CO_2 vibrational energy escapes through the bend mode. More than half of this energy is transferred to the CCl_2 symmetric stretch mode (715 cm^{-1}). The remaining energy is accepted by other modes with frequencies close to the CO_2 bend vibration (CH_2 rocking at 898 cm^{-1} and CCl_2 asymmetric stretch at 769 cm^{-1}). 27% of the CO_2 excess energy is transferred from the symmetric stretch (1350 cm^{-1}) to nearby solvent modes at 1153, 1270, and 1434 cm^{-1}.

6. Acknowledgements

AK gratefully acknowledges support by the Deutsche Forschungsgemeinschaft.

References

1 A. Laubereau and W. Kaiser, *Rev. Mod. Phys.*, 1978, **50**, 607.
2 D. W. Oxtoby, *Adv. Chem. Phys.*, 1981, **47**, 487.
3 J. Chesnoy and G. M. Gale, *Adv. Chem. Phys.*, 1988, **70**, 297.
4 H. Hippler and J. Troe, in *Bimolecular Collisions*, ed. M. N. R. Ashfold and J. E. Baggot, Royal Society of Chemistry, London, 1989, pp. 209–262.
5 T. Elsaesser and W. Kaiser, *Annu. Rev. Phys. Chem.*, 1991, **42**, 83.
6 R. M. Whitnell, K. R. Wilson and J. T. Hynes, *J. Chem. Phys.*, 1992, **96**, 5354.
7 J. C. Owrutsky, D. Raftery and R. M. Hochstrasser, *Annu. Rev. Phys. Chem.*, 1994, **45**, 519.

8 G. Flynn, C. Parmenter and A. M. Wodtke, *J. Phys. Chem.*, 1996, **100**, 12817.
9 R. M. Stratt and M. Maroncelli, *J. Phys. Chem.*, 1996, **100**, 12891.
10 D. Schwarzer, J. Troe and M. Zerezke, *J. Chem. Phys.*, 1997, **107**, 8380.
11 J. C. Deak, L. K. Iwaki and D. D. Dlott, *J. Phys. Chem. A*, 1999, **103**, 971.
12 C. G. Elles, D. Bingemann, M. M. Heckscher and F. F. Crim, *J. Chem. Phys.*, 2003, **118**, 5587.
13 C. P. Lawrence and J. L. Skinner, *J. Chem. Phys.*, 2003, **119**, 1623.
14 M. Teubner and D. Schwarzer, *J. Chem. Phys.*, 2003, **119**, 2171.
15 R. Rey, K. B. Moller and J. T. Hynes, *Chem. Rev.*, 2004, **104**, 1915.
16 D. Schwarzer, J. Lindner and P. Vöhringer, *J. Phys. Chem. A*, 2006, **110**, 2858.
17 Y. Kimura, Y. Yamamoto, H. Fujiwara and M. Terazima, *J. Chem. Phys.*, 2005, **123**, 054512.
18 Y. Kimura, Y. Yamamoto and M. Terazima, *J. Chem. Phys.*, 2005, **123**, 054513.
19 L. K. Iwaki and D. D. Dlott, *J. Phys. Chem. A*, 2000, **104**, 9101.
20 D. D. Dlott, *Chem. Phys.*, 2001, **266**, 149.
21 V. N. Kabadi and B. M. Rice, *J. Phys. Chem. A*, 2004, **108**, 532.
22 P. B. Graham, K. J. Matus and R. M. Stratt, *J. Chem. Phys.*, 2004, **121**, 5348.
23 D. Laage, H. Demirdjian and J. T. Hynes, *Chem. Phys. Lett.*, 2005, **405**, 453.
24 A. Kandratsenka, J. Schroeder, D. Schwarzer and V. S. Vikhrenko, *Phys. Chem. Chem. Phys.*, 2005, **7**, 1205.
25 M. Buback, M. Kling, S. Schmatz and J. Schroeder, *Phys. Chem. Chem. Phys.*, 2004, **6**, 5441.
26 J. Aschenbruecker, M. Buback, N. P. Ernsting, J. Schroeder and U. Steegmueller, *J. Phys. Chem. B*, 1998, **102**, 5552.
27 J. Aschenbruecker, M. Buback, N. P. Ernsting, J. Schroeder and U. Steegmueller, *Ber. Bunsen-Ges. Phys. Chem.*, 1998, **102**, 965.
28 M. Buback, M. Kling, M. T. Seidel, F.-D. Schott, J. Schroeder and U. Steegmueller, *Z. Phys. Chem.*, 2001, **215**, 717.
29 C. Heidelbach, D. Schwarzer, J. Schroeder and V. S. Vikhrenko, *Chem. Phys. Lett.*, 1998, **291**, 333.
30 C. Heidelbach, V. S. Vikhrenko, D. Schwarzer and J. Schroeder, *J. Chem. Phys.*, 1999, **110**, 5286.
31 C. Eckart, *Phys. Rev.*, 1935, **47**, 552.
32 B. Wilson Jr, J. C. Decius and P. C. Cross, *Molecular vibrations: The theory of infrared and Raman vibrational spectra*, McGraw-Hill, New York, 2nd edn, 1966.

